

# Integrating Absorption Technologies for Cooling and Waste Heat Upgrading in Data Centers

*Konrad Ostermann<sup>1\*</sup>, Ludwig Irrgang<sup>1</sup>, Hartmut Spliethoff<sup>1</sup>, Christopher Schiffelechner<sup>1</sup>*

<sup>1</sup>*Chair of Energy Systems, Technical University of Munich, Munich, Germany*

*\*Corresponding Author: konrad.ostermann@tum.de*

## Abstract:

The increasing power density of modern data centers, driven by artificial intelligence and high-performance computing workloads, results in a substantial rise in cooling energy demand and waste heat generation. This work investigates the integration of absorption machines into data center cooling infrastructures as a thermally driven alternative to conventional electrically operated systems. Two system types are considered: the absorption chiller (AC), which enables the replacement of vapor compression chillers using thermal driving energy from sources such as industrial waste heat or geothermal energy, and the absorption heat transformer (AHT), which upgrades data center waste heat to a higher temperature level for feed-in into district heating networks. Steady-state models based on mass and energy balances are adapted for both systems using the H<sub>2</sub>O/LiBr working fluid pair, and the operational limits are characterized as a function of external temperature boundary conditions. The models are applied to two representative reference data centers, a hybrid air-water-cooled facility and an immersion-cooled facility, in annual simulations using hourly meteorological data from the Munich area. For the AC, a design generator temperature of 95 °C is identified to ensure year-round operability, yielding an annual utilization of 61.9 % with a moderate seasonal COP variation of 5.71 %. For the AHT, waste heat at 65 °C is shown to be sufficient to meet the 80 °C district heating supply requirement for ambient temperatures below 24 °C, resulting in a high annual utilization of 93.45 % and a seasonal COP variation of only 2.63 %.

## Keywords:

Absorption chiller; Absorption heat transformer; Data center cooling; Geothermal energy; Waste heat utilization; District heating;

## 1 Introduction

The global digital transformation has led to a massive expansion of data processing capacities, with worldwide data volumes having already reached 175 zettabytes in 2025 [1]. Data centers form the infrastructural backbone of this development. The landscape ranges from small edge data centers at the network periphery and enterprise-internal facilities to massive hyperscale installations operated by major technology corporations [2, 3]. The continuing trend toward outsourcing has resulted in more than 55 % of IT workloads being migrated to external colocation or cloud environments [3, 4].

A key driver of this development is the rapid increase in power density per rack, driven by the growing demands of artificial intelligence (AI), machine learning, and high-performance computing (HPC) [1, 4]. While the industry-wide average rack density still lies at approximately 7.1 to 8 kW, configurations in the range of 15 to 29 kW are becoming increasingly prevalent [4]. In specialized high-performance environments, densities of 30 kW are already established, with state-of-the-art GPU servers for AI applications capable of exceeding 100 kW per rack [5]. This trend is closely linked to advances in microprocessor technology: the thermal design power (TDP) of high-performance CPUs surpassed 700 W in 2025 [1], increasingly pushing conventional air-based cooling systems to their physical limits.

This technological evolution results in a dramatic increase in the global electricity demand of data centers. In the United States, for example, energy consumption doubled between 2013 and 2020 from 70 to 140 TWh and rose further to an estimated 176 TWh by 2023, already accounting for 4.4 % of total national consumption [3, 6]. Globally, data centers are projected to account for approximately 4.5 % of worldwide energy consumption by 2026 [1]. Since virtually all electrical energy consumed is ultimately converted into heat, and cooling systems

can already account for up to 40 % of a data center’s total energy consumption [1, 5], the development of highly efficient thermal management solutions is of extreme importance.

To quantify the energy efficiency of data centers, the Power Usage Effectiveness (PUE) has become established as a global industry standard. This metric describes the ratio of the total energy demand of the facility to the power consumption of the IT equipment, with a value of 1.0 representing the theoretical ideal of zero infrastructure losses [2]. Despite technological advances, the global average PUE has stagnated at approximately 1.55 to 1.56 in recent years [1, 4, 5], underscoring the need to develop thermal concepts beyond conventional approaches in order to reduce operational costs and minimize environmental impact.

In response to this substantial energy demand, governments are increasingly intervening through regulation. Germany has established a binding framework with the Energy Efficiency Act (Energieeffizienzgesetz, EnEFG), enacted in 2023 [7]. The EnEFG stipulates that data centers must achieve an annual average PUE of no more than 1.5 from July 2027 and a sustained value of 1.3 from July 2030 onward. In addition, waste heat utilization is gaining regulatory prominence. For new facilities commencing operation from July 2026, a minimum reused energy share of 10 % is mandated, rising to 20 % for projects commissioned from 2028 onward. These regulatory requirements make clear that future data centers must be fundamentally reconceived with regard to both cooling efficiency and waste heat utilization.

As an alternative to conventional electrically driven systems, in particular vapor compression chillers and heat pumps, sorption technologies offer a promising approach, as they are driven primarily by thermal energy and increase the electrical energy demand of the data center only marginally. The integration of adsorption systems into data centers has already been investigated in [8]. Absorption machines, which are the focus of the present work, are distinguished from adsorption systems by their continuous operation, higher power density and higher efficiencies [9, 10], making them a particularly suitable option for deployment in data centers. Two types of absorption machines can be distinguished, each relevant to different application scenarios in data centers.

On the one hand, the absorption chiller (AC) enables the replacement of conventional electrically driven vapor compression chillers. The AC is driven by thermal energy, which can be supplied, for example, from industrial waste heat streams or geothermal sources [11], thereby allowing the electrical energy demand associated with cooling to be nearly entirely eliminated. Geothermal heat sources are of particular interest in this context, as they provide a stable, weather-independent thermal driving input throughout the year. This application is particularly relevant for data centers requiring supply cooling temperatures in the range of 4 to 35 °C [12]. On the other hand, the absorption heat transformer (AHT) offers the capability to upgrade the waste heat of a data center to a higher temperature level for productive use. In comparison to vapor compression heat pumps, the electrical energy demand of the AHT is virtually negligible, as the transformation process is thermally driven. The AHT is suitable for data centers with waste heat temperatures of at least 55 °C [12] and enables the feed-in of the transformed heat into district heating networks or industrial processes.

The objective of the present work is the systematic investigation of the integration of absorption machines into data centers. To this end, models for the AC and AHT are adapted, enabling the characterization of operational limits and thermodynamic performance as a function of external temperature levels. On the basis of these models, integration strategies are elaborated for two representative reference data centers and evaluated by means of annual simulations incorporating real meteorological data. The results are intended to demonstrate under which conditions the deployment of absorption machines in data centers is thermodynamically viable and what potential exists for reducing electrical energy consumption and utilizing waste heat.

## 2 Cooling Systems in Data Centers

Thermal management in data centers is primarily achieved through air- or liquid-based cooling systems, with the choice of system largely determined by rack power density and operational requirements with regard to efficiency and waste heat utilization [13]. While conventional air cooling dissipates heat at the room, row, or rack level, these systems are increasingly reaching their physical limits with modern high-performance chips [1]. More efficient alternatives include rear door heat exchangers (RDHx) and direct liquid cooling (DLC), in which the cooling medium is routed via cold plates directly to heat-intensive IT components such as CPUs and GPUs [1, 14]. Maximum heat removal density is achieved through immersion cooling, in which the hardware is fully submerged in a dielectric fluid [15]. In practice, hybrid architectures are becoming increasingly prevalent, combining DLC for processors with supplementary air cooling for peripheral components [1].

A prominent trend is the deliberate elevation of coolant temperatures in order to maximize the operating hours in free cooling mode and to increase the thermodynamic quality of waste heat for downstream utilization. Modern liquid cooling systems can tolerate supply temperatures of 50 °C to above 70 °C [1]. However, this strategy is constrained by technical trade-offs: higher operating temperatures lead to increased leakage currents in semiconductors, which

can raise the power consumption of IT components by approximately 1 % to 5 % per 10 K temperature increase [16]. Furthermore, exceeding critical temperature thresholds risks thermal throttling, in which processors reduce their clock frequency, resulting in a significant drop in computing performance. [16]

The required cooling capacity is provided through various thermal sources. Conventional systems rely on mechanical vapor compression chillers, which account for a substantial share of the total energy consumption of a data center [14, 17]. To improve efficiency, free cooling is increasingly employed, in which ambient air or natural water sources are used directly for heat rejection without mechanical refrigeration. The combination of both approaches in hybrid systems allows free cooling to be prioritized, with compressor-based operation confined to periods of elevated ambient temperatures [2, 3].

Beyond conventional cooling solutions, alternative cooling infrastructures are attracting growing interest as a means of further improving energy efficiency and expanding waste heat utilization options [17, 18]. In the context of studying integration strategies, reference data centers are to be selected. Since the choice of cooling system depends on a wide range of operational and structural boundary conditions and no universally optimal system can be defined, two representative reference data centers with fundamentally different cooling architectures are considered.

### **Reference Data Center 1: Hybrid Air-Water-Cooled Data Center**

The first reference data center is Building 725E of Sandia National Laboratories in Albuquerque, New Mexico, completed in 2018 [14]. The facility is designed for an IT load of up to 14 MW at full buildout, is LEED v4 Gold certified, and has achieved an annual average PUE of approximately 1.10 [14]. The cooling concept is based on a hybrid air-water architecture with three hydraulically decoupled circuits: a chilled water loop (CW,  $\approx 14^\circ\text{C}$ ) serving the free cooling system and vapor compression chiller, a medium-temperature water loop (MTW,  $\approx 15.5^\circ\text{C}$ ) supplying the air-handling units of the data hall, and a process water loop (PW,  $\approx 24.5^\circ\text{C}$ ) serving the direct liquid cooling systems of the IT components [14]. Approximately 85 % of the data center's heat load is rejected via liquid cooling.

For the following investigations, the operating strategy is adopted whereby the data center is operated exclusively in free cooling mode at ambient temperatures below  $8^\circ\text{C}$  and switches to chiller-based operation above this threshold. The supply temperature of the CW loop of  $14^\circ\text{C}$  is used as the governing cooling temperature for the AC integration.

### **Reference Data Center 2: Immersion-Cooled Data Center**

The second reference data center is based on the patented Hybrid Immersion Liquid Cooling concept by OVHcloud [19], which combines passive single-phase immersion cooling with direct-to-chip liquid cooling. Servers are submerged in individual tanks filled with a non-conductive dielectric fluid, while CPUs and GPUs are additionally connected via water cold plates to an external pumping circuit. No fans or pumps are required at the rack or server level, reducing the electrical cooling overhead and enabling higher packing densities.

The thermodynamically decisive feature of this concept is the achievable return temperature of the data center water circuit of up to  $65^\circ\text{C}$  [19], which substantially facilitates the economic utilization of waste heat through heat transformation systems. Heat rejection to the environment is handled as standard by external dry coolers operating in free cooling mode. OVHcloud reports a reduction in cooling energy consumption of at least 20 % compared to conventional water cooling, as well as a partial PUE (PPUE) of 1.004 [19]. For the following investigations, the return temperature of  $65^\circ\text{C}$  is adopted as the waste heat temperature and thus as the evaporator and generator temperature of the AHT.

## **3 Absorption Technology for Heat Dissipation**

This section introduces the thermodynamic principles of absorption heat pumps and describes the steady-state models adapted for the AC and AHT. The modeling framework, including the treatment of external heat rejection via dry coolers, forms the basis for the performance analyses presented in the subsequent sections.

### **3.1 Absorption Technology**

Absorption heat pumps are comparable in their fundamental design to vapor compression systems. As illustrated in Figure 1, Type 1 (a) represents the configuration of an absorption chiller (AC) and Type 2 (b) that of an absorption heat transformer (AHT). Both types share the common feature of incorporating a condenser and an evaporator, analogous to vapor compression systems. The key difference lies in the replacement of an electrically driven mechanical compressor by a thermal compressor, which consists of a generator, an absorber, an internal heat exchanger (solution heat exchanger - SHEX), an expansion valve, and a solution pump.

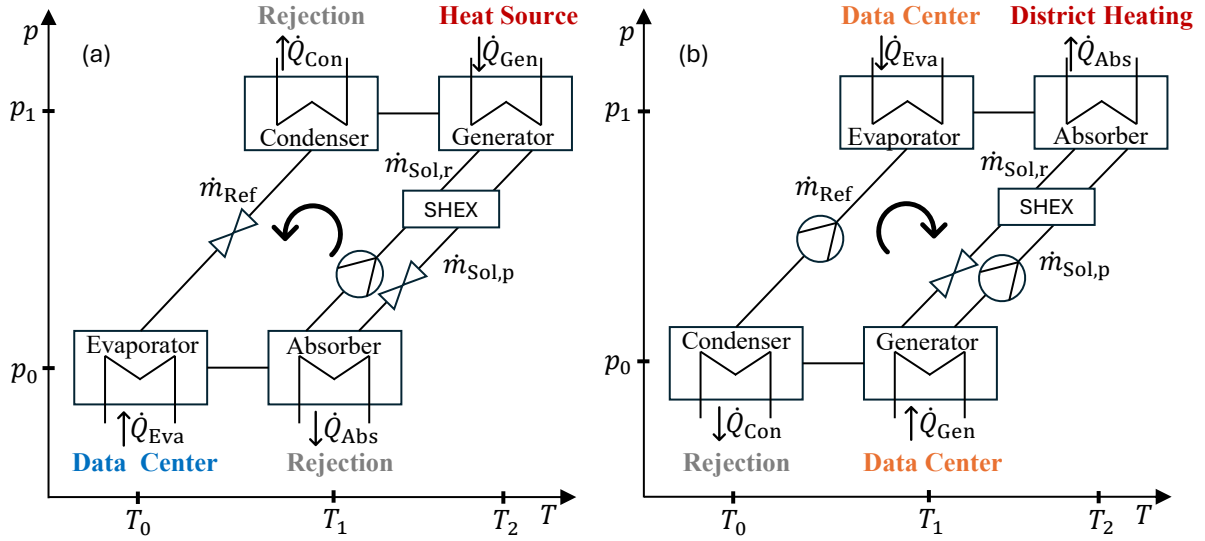


Figure 1: Schematic representation based on the Dühring diagram for the AC (a) and the AHT (b) [12].

As with vapor compression systems, the absorption cycle operates with a refrigerant. In addition, the absorption process requires a solvent in which the refrigerant is periodically absorbed and desorbed. In commercial applications, two working fluid pairs are predominantly used: water/lithium bromide ( $H_2O/LiBr$ ), in which water serves as the refrigerant and  $LiBr$ -solution as the solvent, and ammonia/water ( $NH_3/H_2O$ ), in which ammonia acts as the refrigerant and water as the solvent. For the analysis of integrating absorption systems into data centers, only the working fluid pair  $H_2O/LiBr$  is considered, as it is well suited to the relevant temperature levels and is widely established in industrial applications [20].

The absorption heat pump comprises four main components: the condenser and evaporator as pure heat exchangers, and the generator and absorber as components involving combined heat and mass transfer. In the pressure-temperature diagram ( $p$ - $T$  diagram), three distinct temperature levels are identifiable, which must be supplied or served by the system. The two pressure levels are defined by the saturation pressure of the refrigerant at the condensation and evaporation temperatures, respectively. The refrigerant vapor migrates from the high-pressure side to the low-pressure side under the prevailing pressure difference, while the solution circuit, comprising absorber, solution pump, generator, and expansion valve, collectively assumes the function of the mechanical compressor in conventional vapor compression systems.

Regarding the thermodynamic cycle, the AC and AHT differ fundamentally. The AC operates as a left-handed cycle, in which driving heat is supplied at a high temperature level to provide cooling at a low temperature level. The AHT, by contrast, operates as a right-handed cycle, in which waste heat supplied at a medium temperature level is upgraded to a higher temperature level. Due to the reversed flow direction of the solution, the AHT requires a pump between the condenser and evaporator instead of an expansion valve. [12]

In addition to the basic *single-effect, single-lift* configuration shown in Figure 1, absorption systems can also be realized in *double-effect* or *double-lift* configurations. In the *double-lift* configuration, a second low-pressure stage is added, enabling the utilization of lower source temperatures, but at the cost of reduced efficiency. The *double-effect* configuration incorporates an additional high-pressure stage, allowing for higher efficiency when elevated driving temperatures are available [20]. In the present work, only *single-effect, single-lift* systems are considered, as the available external heat source temperature levels and the targeted temperature lift of the AHT have been identified as sufficient. For other application scenarios, however, the investigation of alternative system configurations may be appropriate.

To characterize the efficiency of an absorption system, the coefficient of performance (COP) is used, which describes the ratio of useful heat output to the heat input supplied. For the AC, the  $COP_{AC}$  is defined in Equation 1 as the ratio of the useful cooling capacity at the evaporator  $\dot{Q}_{Eva}$  to the driving heat input at the generator  $\dot{Q}_{Gen}$ .

$$COP_{AC} = \frac{\dot{Q}_{Eva}}{\dot{Q}_{Gen}} \quad (1)$$

For the AHT, the  $COP_{AHT}$  is defined in Equation 2 as the ratio of the useful heat output at the absorber  $\dot{Q}_{Abs}$  to the total waste heat supplied at the evaporator  $\dot{Q}_{Eva}$  and the generator  $\dot{Q}_{Gen}$ .

$$\text{COP}_{\text{AHT}} = \frac{\dot{Q}_{\text{Abs}}}{\dot{Q}_{\text{Eva}} + \dot{Q}_{\text{Gen}}} \quad (2)$$

Typical COP values for *single-effect* AC systems operating with the H<sub>2</sub>O/LiBr working fluid pair range from 0.6 to 0.9, while AHT systems typically achieve COP values between 0.45 and 0.55 [20].

### 3.2 Absorption Chiller and Heat Transformer Model

To determine the operational limits and thermodynamic performance of the AC and AHT, both processes are modeled based on mass and energy balances. Given the external inlet temperatures and the required thermal capacity, the model determines the relevant state variables within the system and calculates the respective COP. The following simplifying assumptions apply to both models:

- Heat exchangers are modeled using pinch temperature approaches
- Steady-state operation
- Saturated vapor at the evaporator outlet
- Saturated liquid at the condenser outlet
- Saturated solution at the outlets of generator and absorber
- Pressure losses are neglected
- Heat losses to the environment are neglected
- Constant heat capacity in the solution heat exchanger (SHEX)
- Refrigerant temperature at the generator outlet is 5 K below the generator temperature

The AC model is based on existing mass and energy balances from [21], which are available as an open-source implementation [22] and have been adapted for the present application. The system configuration follows the layout shown in Figure 1. The thermodynamic properties of the H<sub>2</sub>O/LiBr working fluid mixture in the generator and absorber are calculated using the formulations from [23]. The thermophysical properties of the refrigerant H<sub>2</sub>O are determined using the CoolProp library [24]. In addition to the pinch temperatures, the model verifies compliance with the crystallization limit of the working fluid mixture and determines the solution concentration in the generator and absorber.

The AHT model is based on the same governing equations, with the mass and energy balances adapted to reflect the right-handed cycle configuration. A pump replaces the expansion valve between the condenser and evaporator. The thermophysical properties are calculated analogously to the AC model using [23] and CoolProp [24]. The model parameters are summarized in Table 1.

Table 1: Assumed model parameters for AC and AHT

Parameter	Value	Unit
Pinch temperature evaporator $\Delta T_{\text{Eva}}$	5	K
Pinch temperature absorber $\Delta T_{\text{Abs}}$	5	K
Pinch temperature generator $\Delta T_{\text{Gen}}$	5	K
Pinch temperature condenser $\Delta T_{\text{Con}}$	5	K
Pinch temperature SHEX $\Delta T_{\text{SHEX}}$	5	K
Pump efficiency $\eta_{\text{pump}}$	95	%

For most heat exchangers, the external inlet temperatures are directly prescribed by the heat source or demand side. An exception is the heat rejection temperature, which applies at the condenser and absorber of the AC and at the condenser of the AHT. This temperature is not determined by the process itself but by the external heat rejection system, and is primarily dependent on ambient conditions.

Various system types are generally available for heat rejection in absorption systems, including wet cooling towers, evaporative condensers, hybrid coolers, and dry coolers. In the context of integration into data centers, only dry coolers are considered in the following. Dry coolers are air-cooled heat exchangers in which the cooling medium flows through finned tubes and heat is dissipated exclusively by convective heat transfer to the ambient air. Since no evaporation takes place, the achievable heat rejection temperature is directly coupled to the outdoor air temperature, which directly affects the thermodynamic performance of the absorption system.

To represent this relationship in the model, a constant pinch temperature difference of 6 K between the ambient air temperature and the heat rejection temperature is assumed in Equation 3 following [25]:

$$T_{\text{RC}} = T_{\text{amb}} + \Delta T_{\text{RC}} \quad (3)$$

where  $T_{RC}$  denotes the heat rejection temperature,  $T_{amb}$  the ambient air temperature, and  $\Delta T_{RC} = 6$  K the assumed pinch temperature difference of the dry cooler. This correlation allows time-resolved ambient air temperatures to be directly passed as input to the model, enabling the seasonal variability of the heat rejection temperature to be accounted for in the assessment of system performance.

## 4 Performance Analysis and Integration of Absorption Technology in Data Centers

Using the models adapted in Section 3.2, the operational limits of the AC and AHT are first determined in order to characterize both systems and define the feasible operating ranges for their integration into data centers. For this purpose, the temperature ranges in which each system can be operated are identified. Based on the resulting design temperatures, both systems are subsequently integrated into the respective reference data centers within two dedicated use cases, and their annual operating behavior is analyzed by means of a time-resolved simulation.

### 4.1 Operating Limits

Using the models described in Section 3.2, the operational limits of the AC and AHT are characterized. These serve to define the feasible operating ranges of the respective absorption technology for data center applications. The characterizing parameters are the external temperature levels at which heat is supplied to or rejected from the system. For the AC, the relevant temperatures are the driving temperature at the generator, the heat rejection temperature at the condenser and absorber, and the required cooling temperature at the evaporator. For the AHT, the governing parameters are the waste heat temperature of the data center at the evaporator and generator, the heat rejection temperature at the condenser, and the target useful heat temperature at the absorber. The resulting operational limits for the AC (a, b) and the AHT (c, d) are shown in Figure 2.

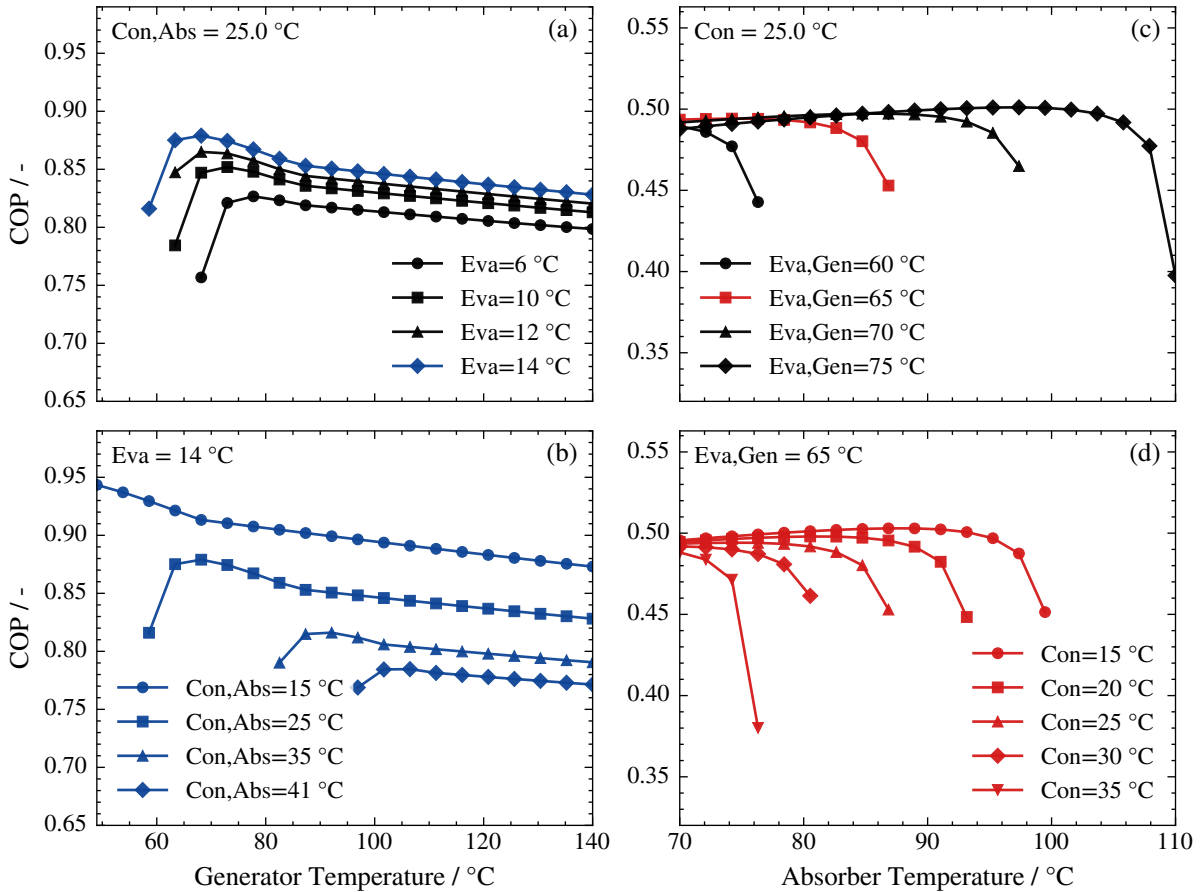


Figure 2: Operational limits and COP characteristics for the AC (a, b) and the AHT (c, d) as a function of the external temperature levels.

#### 4.1.1 Operational Limits of the Absorption Chiller

To characterize the operational limits of the AC, a constant heat rejection temperature of 25 °C is initially assumed and the COP is calculated as a function of the generator temperature for various evaporator temperatures. The results are shown in Figure 2 (a). As expected, the COP decreases with falling evaporator temperature, since lower

evaporation temperatures require a larger pressure difference to be overcome between the low- and high-pressure sides, which demands a higher driving input at the generator and thus worsens the ratio of useful output to driving input. Furthermore, it is evident that the AC cannot be operated below a certain minimum generator temperature. This minimum generator temperature depends on the evaporator temperature considered and lies in the range of 60 to 80 °C for a condenser and absorber temperature of 25 °C.

It is further observed that the COP passes through a maximum as the generator temperature increases and subsequently declines. This behavior is attributed to the disproportionate increase in the driving heat input  $\dot{Q}_{\text{Gen}}$  at elevated generator temperatures, while the useful cooling capacity at the evaporator  $\dot{Q}_{\text{Eva}}$  remains prescribed by the cooling demand and does not increase proportionally. From a thermodynamic perspective, the increasing temperature differences across the heat exchangers at higher generator temperatures give rise to greater irreversible losses, further reducing the achievable efficiency relative to the reversible limiting case. It follows that, under otherwise constant operating conditions, the generator temperature should always be chosen as low as possible to achieve the highest COP.

As the reference data center, an air-cooled data center [14] as described in Section 2 is considered, which operates with a cooling water supply temperature of 14 °C. This yields a design evaporator temperature of 14 °C, which is highlighted in Figure 2 (a). Since this evaporator temperature can be assumed constant under normal operating conditions, the influence of the heat rejection temperature on the COP and operational limits is investigated in Figure 2 (b). In the AC, the heat rejection temperature, as described in Section 3.2, is directly coupled to the ambient air temperature when dry coolers are used. It can therefore not be assumed constant, and daily as well as seasonal variations in ambient temperature must be accounted for in the system design.

Figure 2 (b) shows the COP as a function of the generator temperature for a constant evaporator temperature of 14 °C and condenser and absorber temperatures ranging from 15 to 41 °C. The operational limits exhibit a strong dependence on the heat rejection temperature. While a heat rejection temperature of 15 °C allows generator temperatures as low as 45 °C to sustain AC operation, a heat rejection temperature of 41 °C requires a minimum generator temperature of 95 °C. Furthermore, the achievable COP values decrease significantly with increasing heat rejection temperature. The elevated condensation pressure at higher heat rejection temperatures increases the vapor fraction generated during expansion across the expansion valve, reducing the effective specific cooling capacity and demanding a disproportionately higher driving heat input at the generator. In this case as well, it is confirmed that the generator temperature should be chosen as low as possible for any given heat rejection temperature in order to maximize the COP.

Based on this operational limits analysis, the design generator temperature for the reference data center is established. The design criterion requires that AC operation can be ensured throughout the entire year. As Munich is assumed to be the location of the data center, a maximum ambient air temperature of 35 °C is assumed. Should this value be exceeded, a vapor compression chiller is activated as a redundant parallel system to ensure the operational reliability of the data center, since uninterrupted cooling must be guaranteed at all times. Accounting for the pinch temperature difference of 6 K between ambient air and heat rejection temperature specified in Section 3.2, a maximum condenser and absorber temperature of 41 °C is obtained. To ensure AC operation even under these worst-case heat rejection conditions, the system is designed for a generator temperature of 95 °C.

#### 4.1.2 Operational Limits of the Absorption Heat Transformer

The operational limits of the AHT are shown in Figure 2 (c) and (d). Analogously to the approach taken for the AC, a constant condenser temperature of 25 °C is initially assumed. The COP is calculated as a function of the absorber temperature, which corresponds to the useful heat output temperature, for various evaporator and generator temperatures. These represent the waste heat temperatures of the data center supplied to the AHT as the driving input.

As expected, it is evident that higher waste heat temperatures at the evaporator and generator enable higher absorber temperatures to be achieved. The attainable temperature lift between the supplied waste heat and the transformed useful heat increases with rising waste heat temperature. This behavior is rooted in the thermodynamic equilibrium of the H<sub>2</sub>O/LiBr working fluid pair: higher evaporator and generator temperatures result in an elevated system pressure on the high-pressure side of the AHT. Since the maximum achievable absorber temperature is governed by the solution equilibrium and thus primarily by the prevailing high-side pressure, higher waste heat temperatures enable both a higher absorber temperature and a greater usable temperature lift.

For further characterization of the operational limits, the AHT is analyzed based on a concrete application case. The reference data center is an immersion-cooled data center [19] as described in Section 2, operating with a waste heat temperature of 65 °C. This evaporator and generator temperature of 65 °C is assumed constant and is highlighted in Figure 2 (d). Analogously to the AC analysis, the influence of the heat rejection temperature on the COP and operational limits is investigated in a second step. The COP is calculated as a function of the absorber

temperature for condenser temperatures ranging from 15 to 35 °C.

A pronounced dependence of both the operational limits and the system performance on the heat rejection temperature is observed. As the condenser temperature increases, the maximum achievable absorber temperature decreases, since a higher condenser pressure reduces the driving force for refrigerant absorption in the absorber and thereby limits the attainable useful heat temperature level. Simultaneously, the achievable COP values decline with increasing heat rejection temperature, as the usable temperature differences within the process are reduced.

Based on this operational limits analysis, the design parameters for the reference data center are established. The evaporator and generator temperature is fixed at 65 °C by the waste heat of the data center. The AHT is integrated into the data center with the objective of upgrading the available waste heat to a higher temperature level for feed-in into a district heating network. The district heating network operates at a constant supply temperature of 80 °C [26], which imposes the requirement that the absorber temperature must reach at least 80 °C. From Figure 2 (d), it is apparent that this condition can only be satisfied if the heat rejection temperature does not exceed 30 °C. Accounting for the pinch temperature difference of 6 K between ambient air and heat rejection temperature specified in Section 3.2, this corresponds to a maximum permissible ambient air temperature of 24 °C for year-round AHT operation with district heating feed-in. During periods in which this temperature threshold is exceeded, the data center reverts to pure free cooling operation. In this setup, the installed dry coolers serve both the heat rejection demand of the AHT and the free cooling supply of the data center.

## 4.2 Integration Strategies for Absorption Technology in Data Centers

The integration of an AC and an AHT into data center cooling infrastructures is analyzed by means of an annual simulation. The two reference data centers introduced in Section 2 serve as the basis for the respective use cases. The simulation accounts for the operational limits and design parameters determined in the preceding sections. Hourly recorded weather data from the Munich area are used for the time-resolved annual calculation in order to analyze the influence of ambient temperature on the heat rejection temperature and, consequently, on system performance throughout the year.

### 4.2.1 Use Case: Integration of the Absorption Chiller

In the first use case, an AC is integrated into the cooling infrastructure of the air-cooled reference data center introduced in Section 2. The essential operating parameters are prescribed by the boundary conditions of the data center. The cooling demand determines the evaporator temperature at 14 °C, and the operational limits analysis presented in Section 4.1.1 yields a design generator temperature of 95 °C. Both temperatures are assumed constant throughout the annual simulation. The remaining input variable is the heat rejection temperature at the condenser and absorber, which is derived from the pinch temperature approach described in Section 3.2 applied to the hourly ambient temperature data of the Munich site.

The integration strategy replaces the conventional vapor compression chiller with the AC, while the remaining cooling infrastructure is left unchanged. Below an ambient temperature of 8 °C, the data center is operated entirely in free cooling mode, as the dry coolers are sufficient to meet the cooling demand directly. The associated minor increase in cooling water temperature due to the pinch temperature difference between ambient and heat rejection temperature remains within the permissible operating limits of the data center. The resulting operating strategy states that the AC is operated exclusively at ambient temperatures of  $T_{\text{amb}} \geq 8 \text{ °C}$  and is shut down at lower temperatures.

For the annual simulation, it is checked for each hour whether the ambient temperature exceeds the threshold of 8 °C and AC operation is required. If so, the heat rejection temperature is derived from the ambient temperature and the hourly COP of the system is calculated accordingly. This procedure is repeated for all 8760 hours of the year. The results of the annual simulation are shown in Figure 3. In addition to the monthly averaged ambient temperatures, the monthly operational utilization of the system is given in percent, representing the share of operating hours relative to the total hours of the respective month. Furthermore, the monthly averaged COP values are presented, computed exclusively over the hours during which the system was in operation.

The results show that the operational utilization of the AC is considerably lower in the winter months than in the summer months. Over the entire year, a total operating duration of 5421 hours is obtained, corresponding to an annual utilization of 61.9 %. It should be noted that the operating hours of the AC in this use case are equivalent to those of the replaced vapor compression chiller in the conventional system, as both systems serve the same cooling demand and are subject to the same switching constraint governing the transition to free cooling operation.

Furthermore, the monthly averaged COP exhibits a seasonal dependence consistent with the results of the operational limits analysis presented in Figure 2. In the summer months, the COP decreases as a result of elevated heat rejection temperatures. This behavior represents a well-known inherent disadvantage of absorption chillers. System efficiency decreases precisely during the months of highest cooling demand. Nevertheless, the seasonal

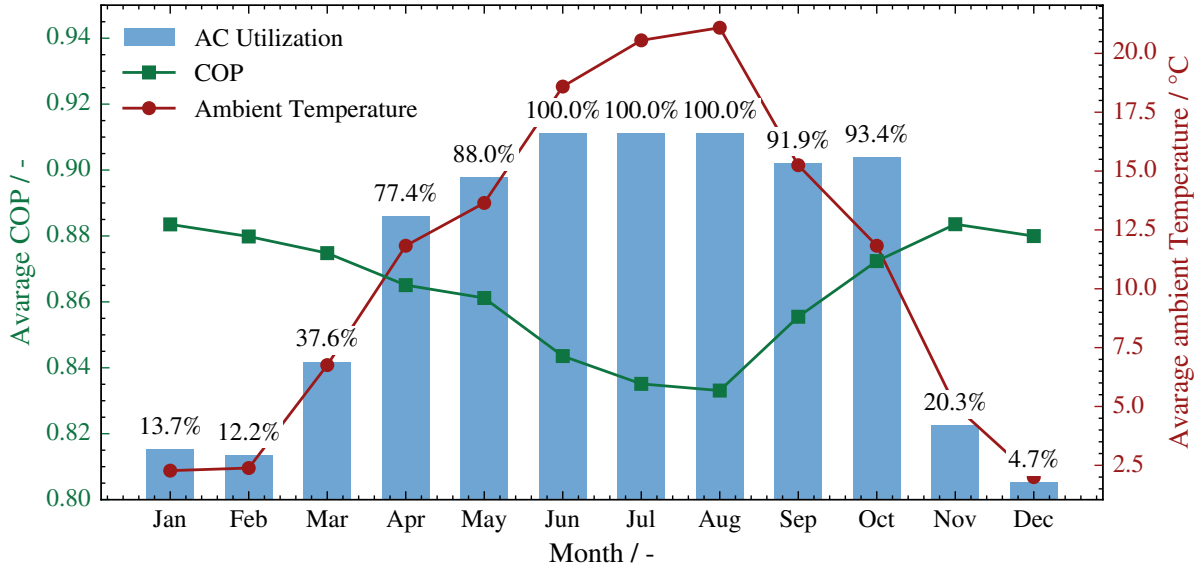


Figure 3: Results of the annual simulation for the integration of the AC into the air-cooled reference data center: monthly averaged ambient temperature, operational utilization, and mean COP.

influence on the COP is moderate in magnitude, as the mean COP values in the summer months deviate from those in the winter months by a maximum of 5.71 %.

#### 4.2.2 Use Case: Integration of the Absorption Heat Transformer

In the second use case, an AHT is integrated into the cooling infrastructure of the immersion-cooled reference data center introduced in Section 2. The waste heat temperature of the data center defines the evaporator and generator temperature at 65 °C. As outlined in Section 4.1.2, the transformed waste heat is fed into a district heating network operating at a constant supply temperature of 80 °C [26]. This temperature corresponds to the required absorber temperature and thus constitutes a further fixed boundary condition. The remaining input variable, the heat rejection temperature at the condenser, is derived analogously to the AC use case from the hourly ambient temperature data of the Munich site.

In contrast to the AC use case, in which the vapor compression chiller is entirely replaced, the AHT represents an extension of the existing free cooling system of the immersion-cooled data center. Under standard operation, the entire waste heat of the data center is rejected to the environment via dry coolers. Through the integration of the AHT, a portion of this waste heat is utilized to provide useful heat for the district heating network, simultaneously reducing the amount of heat to be dissipated to the environment and the associated power demand of the free cooling system. The dry coolers used for free cooling can equally serve as the heat rejection system for the AHT condenser, enabling shared use of the existing infrastructure. As established in the operational limits analysis in Section 4.1.2, AHT operation is restricted to ambient temperatures of  $T_{\text{amb}} \leq 24$  °C, since above this threshold the maximum permissible condenser temperature of 30 °C is exceeded and the required absorber temperature of 80 °C can no longer be achieved. At ambient temperatures above 24 °C, the data center is operated exclusively in free cooling mode.

For the annual simulation, it is checked for each hour whether the ambient temperature falls below the threshold of 24 °C and AHT operation is feasible. If the condition is met, the heat rejection temperature is determined from the ambient temperature and the hourly COP of the AHT is calculated. Analogously to the AC use case, the computed COP values are averaged on a monthly basis and reported together with the monthly operational utilization and the mean ambient temperature. The results of the simulation are presented in Figure 4.

As expected from the inverse operating strategy, the AHT exhibits its highest operational utilization in the winter months, in contrast to the AC, while utilization decreases during the summer. With regard to the feed-in of transformed heat into district heating networks, reduced availability in summer is of limited concern from a systems perspective, as the demand for district heating is substantially lower during the warm season. An extension of operating hours in the summer months, for example through the use of alternative heat rejection systems capable of achieving lower temperatures, is therefore not considered necessary. Over the entire year, a total operating duration of 8186 hours is obtained for the considered site, corresponding to an annual utilization of 93.45 %.

A key advantage of the AHT's operating characteristics relative to those of the AC lies in the fact that the system preferentially operates at low ambient temperatures. This has a favorable effect on the achievable COP values, as the heat rejection temperature and thus the thermodynamic driving effort are low during these periods. Nevertheless,

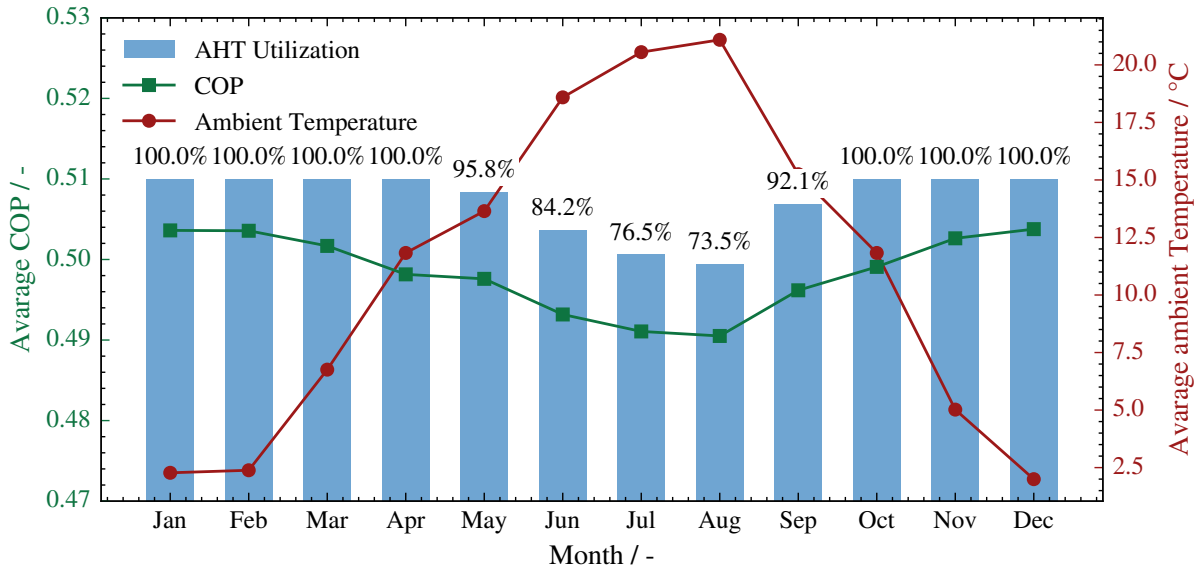


Figure 4: Results of the annual simulation for the integration of the AHT into the immersion-cooled reference data center: monthly averaged ambient temperature, operational utilization, and mean COP.

the seasonal influence of the heat rejection temperature on the COP remains moderate for the AHT. The mean COP values in the winter months deviate from those in the summer months by a maximum of 2.63 %, which is attributed to the comparatively small variation in condenser temperature within the relevant operating range.

## 5 Conclusion

This work investigated the integration of absorption machines into data center cooling infrastructures, focusing on two distinct system types: the absorption chiller (AC) and the absorption heat transformer (AHT). Steady-state models based on mass and energy balances were adapted for both systems using the H<sub>2</sub>O/LiBr working fluid pair, and the operational limits were characterized as a function of external temperature boundary conditions. The models were subsequently applied to two representative reference data centers in annual simulations using hourly meteorological data from the Munich area.

For the AC, the analysis demonstrated that the minimum required generator temperature is strongly dependent on the heat rejection temperature. For the air-cooled reference data center operating at an evaporator temperature of 14 °C, a design generator temperature of 95 °C was identified to ensure year-round operability at the considered site, accounting for a maximum ambient temperature of 35 °C and a dry cooler pinch temperature difference of 6 K. The annual simulation yielded a total operating duration of 5421 hours, corresponding to an annual utilization of 61.9 %. The seasonal variation of the COP, driven by fluctuating heat rejection temperatures, remained moderate, with summer values deviating from winter values by no more than 5.71 %.

For the AHT, the operational limits analysis showed that a waste heat temperature of 65 °C, as provided by the immersion-cooled reference data center, is sufficient to upgrade waste heat to the 80 °C supply temperature required for district heating feed-in. However, this condition is only fulfilled when the heat rejection temperature does not exceed 30 °C, corresponding to a maximum permissible ambient air temperature of 24 °C. The annual simulation yielded a total operating duration of 8186 hours, corresponding to a high annual utilization of 93.45 %. Owing to its inverse seasonal operating profile relative to the AC, the AHT operates preferentially during periods of low ambient temperature, which coincide with elevated district heating demand, a characteristic that renders this integration strategy particularly attractive from both a thermodynamic and a systems perspective. The seasonal COP variation remained within 2.63 %, confirming the robustness of AHT performance across the annual operating range.

The results demonstrate that both absorption machine types represent viable alternatives or complements to conventional electrically driven cooling systems in data centers. The AC offers the potential to nearly entirely eliminate the electrical energy demand for cooling by substituting the vapor compression chiller with a thermally driven system, provided a suitable high-temperature heat source is available. The AHT enables the productive utilization of data center waste heat with negligible additional electrical energy consumption, making it a particularly compelling option for data centers with high waste heat temperatures and proximity to district heating infrastructure.

Future work should extend the present analysis to include a quantitative assessment of the electrical energy savings potential for both integration strategies, as well as an economic evaluation covering capital expenditure, operational costs, and potential revenue from waste heat feed-in. In this context, the coupling of absorption

chillers with geothermal heat sources represents a particularly promising direction, as geothermal energy can serve simultaneously as a year-round driving source for AC operation and as a feed-in source for district heating networks, a synergy that may substantially improve both the economics and the carbon footprint of data center cooling.

## Acknowledgment

We gratefully acknowledge the Bavarian State Ministry of Science and Arts within the framework of the “Geothermal Alliance Bavaria” project for funding.

## Nomenclature

### Abbreviations

Abs	Absorber
AC	Absorption Chiller
AHT	Absorption Heat Transformer
amb	Ambient
Con	Condenser
COP	Coefficient of Performance
CW	Chilled Water Loop
DLC	Direct Liquid Cooling
EnEfG	Energy Efficiency Act
Eva	Evaporator
Gen	Generator
H <sub>2</sub> O	Water
HPC	High-Performance Computing
LiBr	Lithium Bromide
MTW	Medium-Temperature Water Loop
NH <sub>3</sub>	Ammonia
(P)PUE	(Partial) Power Usage Effectiveness
PW	Process Water Loop
RC	Rejection
Ref	Refrigerant
RHDx	Rear Door Heat Exchanger
SHEX	Solution Heat Exchanger
Sol,(r,p)	Solution (rich, poor)
TDC	Thermal Design Power

### Latin Symbols

$\dot{m}$	Mass flow rate, kg/s
$\dot{Q}$	Heat transfer rate, W
$T$	Temperature, °C

### Greek Symbols

$\Delta$	Difference, –
$\eta$	Efficiency, –

## References

- [1] M. Azarifar, M. Arik, and J.-Y. Chang, “Liquid cooling of data centers: A necessity facing challenges,” *Applied Thermal Engineering*, vol. 247, p. 123 112, Jun. 2024, issn: 1359-4311. doi: [10.1016/j.applthermaleng.2024.123112](https://doi.org/10.1016/j.applthermaleng.2024.123112).
- [2] Z. G. M. Setyo, H. B. Rijal, N. Aqilah, and N. Abdullah, “Energy efficiency measurement method and thermal environment in data centers—a literature review,” *Energies*, vol. 18, no. 14, p. 3689, Jul. 2025, issn: 1996-1073. doi: [10.3390/en18143689](https://doi.org/10.3390/en18143689).
- [3] A. Shehabi *et al.*, “2024 united states data center energy usage report,” Lawrence Berkeley National Laboratory, Tech. Rep., 2024. doi: [10.71468/P1WC7Q](https://doi.org/10.71468/P1WC7Q).
- [4] D. Donnellan, A. Lawrence, D. Bizo, P. Judge, and J. O’Brien, “Uptime institute global data center survey 2024,” Uptime Institute, Tech. Rep., 2024. [Online]. Available: <https://uptimeinstitute.com/resources/research-and-reports/uptime-institute-global-data-center-survey-results-2024>.
- [5] S. Bangalore, A. Bhan, A. Del Miglio, P. Sachdeva, V. Sarma, and R. Sharma, “Investing in the rising data center economy,” McKinsey’s Technology, Media and Telecommunications Practice, Tech. Rep., Jan. 2023. [Online]. Available: <https://www.mckinsey.com/industries/technology-media-and-telecommunications/our-insights/investing-in-the-rising-data-center-economy>.
- [6] A. Abbas, A. Huzayyin, T. Mouneer, and S. Nada, “Effect of data center servers’ power density on the decision of using in-row cooling or perimeter cooling,” *Alexandria Engineering Journal*, vol. 60, no. 4, pp. 3855–3867, Aug. 2021, issn: 1110-0168. doi: [10.1016/j.aej.2021.02.051](https://doi.org/10.1016/j.aej.2021.02.051).
- [7] B. Deutschland, *Gesetz zur Steigerung der Energieeffizienz in Deutschland (Energieeffizienzgesetz – enefg)*, Nov. 2023. [Online]. Available: <https://www.gesetze-im-internet.de/eneffg/BJNR1350B0023.html>.

- [8] A. Velte-Schäfer *et al.*, “Utilizing waste heat from data centers with adsorptive heat transformation – heat exchanger design and choice of adsorbent,” *Energy Conversion and Management*, vol. 310, p. 118 500, Jun. 2024, issn: 0196-8904. doi: 10.1016/j.enconman.2024.118500.
- [9] A. Kuczyńska and W. Szaflik, “Absorption and adsorption chillers applied to air conditioning systems,” *Archives of Thermodynamics*, vol. 31, no. 2, pp. 77–94, Jul. 2010, issn: 1231-0956. doi: 10.2478/v10173-010-0010-0.
- [10] R. Wang and R. Oliviera, “Adsorption refrigeration—an efficient way to make good use of waste heat and solar energy,” *Progress in Energy and Combustion Science*, vol. 32, no. 4, pp. 424–458, 2006, issn: 0360-1285. doi: 10.1016/j.peccs.2006.01.002.
- [11] L. Irrgang, C. Frohnwieser, F. Kaufmann, H. Spliethoff, and C. Schiffechner, “Enhanced cold production from geothermal energy using combined absorption and compression cycles,” *International Journal of Refrigeration*, vol. 180, pp. 126–145, Dec. 2025, issn: 0140-7007. doi: 10.1016/j.ijrefrig.2025.08.011.
- [12] F. Cudok, “Gemeinsamkeiten und unterschiede zwischen wärmetransformator- und wärmepumpenprozess,” de, *Technische Universität Berlin (Germany)*, Mar. 2021. doi: 10.14279/DEPOSITONCE-11730.
- [13] Shaos S., Zhang P., and Li X., “Cooling technologies for sustainable data centres. 59th iir technical brief on refrigeration technologies,” *International Institute of Refrigeration (IIR)*, Jan. 2025. doi: 10.18462/IIR.TECHBRIEF.01.2025.
- [14] D. Smith, D. Sickinger, O. Van Geet, and R. Mears, “Sandia national laboratories’ holistic data center design integrates energy- and water efficiency, flexibility, and resilience,” National Renewable Energy Laboratory, Tech. Rep., Jan. 2023. [Online]. Available: <https://docs.nrel.gov/docs/fy23osti/84310.pdf#page=1.00&gsr=0>.
- [15] X. Yuan *et al.*, “Phase change cooling in data centers: A review,” *Energy and Buildings*, vol. 236, p. 110 764, Apr. 2021, issn: 0378-7788. doi: 10.1016/j.enbuild.2021.110764.
- [16] M. Stahlhut, M. Sekulla, P. Großöhme, A. Auweter, and T. Urbaneck, “Data centers with direct liquid-cooled servers: Experimental analysis and modeling,” *Energy Science and Engineering*, vol. 13, no. 7, pp. 3605–3619, Apr. 2025, issn: 2050-0505. doi: 10.1002/ese3.70116.
- [17] K. Ebrahimi, G. F. Jones, and A. S. Fleischer, “A review of data center cooling technology, operating conditions and the corresponding low-grade waste heat recovery opportunities,” *Renewable and Sustainable Energy Reviews*, vol. 31, pp. 622–638, Mar. 2014, issn: 1364-0321. doi: 10.1016/j.rser.2013.12.007.
- [18] X. Chen, X. Wang, T. Ding, and Z. Li, “Experimental research and energy saving analysis of an integrated data center cooling and waste heat recovery system,” *Applied Energy*, vol. 352, p. 121 875, Dec. 2023, issn: 0306-2619. doi: 10.1016/j.apenergy.2023.121875.
- [19] M. Hnayno, J. Jay, and A. Chehade, “New hybrid immersion liquid cooling developments at ovhcloud,” OVHcloud, Tech. Rep., Oct. 2022. [Online]. Available: <https://blog.ovhcloud.com/new-hybrid-immersion-liquid-cooling-developments-at-ovhcloud/>.
- [20] K. E. Herold, *Absorption Chillers and Heat Pumps*, 2nd ed., R. Radermacher and S. A. Klein, Eds. Milton: Taylor and Francis Group, 2016, 1386 pp., Description based on publisher supplied metadata and other sources., isbn: 9781498714358.
- [21] J. Wonchala, M. Hazledine, and K. Goni Boulama, “Solution procedure and performance evaluation for a water–liBr absorption refrigeration machine,” *Energy*, vol. 65, pp. 272–284, Feb. 2014, issn: 0360-5442. doi: 10.1016/j.energy.2013.11.087.
- [22] A. Chidire, L. Irrgang, C. Schiffechner, T. Massier, and A. Romagnoli, “Techno-environmental assessment of geothermal-driven combined cooling and power production,” *Renewable Energy*, vol. 248, p. 122 944, Aug. 2025, issn: 0960-1481. doi: 10.1016/j.renene.2025.122944.
- [23] J. Pátek and J. Klomfar, “A computationally effective formulation of the thermodynamic properties of liBr–h<sub>2</sub>O solutions from 273 to 500k over full composition range,” *International Journal of Refrigeration*, vol. 29, no. 4, pp. 566–578, Jun. 2006, issn: 0140-7007. doi: 10.1016/j.ijrefrig.2005.10.007.
- [24] I. H. Bell, J. Wronski, S. Quoilin, and V. Lemort, “Pure and pseudo-pure fluid thermophysical property evaluation and the open-source thermophysical property library coolprop,” *Industrial and Engineering Chemistry Research*, vol. 53, no. 6, pp. 2498–2508, Jan. 2014, issn: 1520-5045. doi: 10.1021/ie4033999.
- [25] K. M. Katcher, D. Amogne, and A. Patil, “Defining a compact dry cooler design to reduce lcoe contribution in a csp facility,” in *The 2022 International Conference on Battery for Renewable Energy and Electric Vehicles (ICB-REV)*, vol. 2932, AIP Publishing, 2023, p. 110 001. doi: 10.1063/5.0148824.
- [26] S. München, “Fernwärme und rücklauftemperaturin modernen niedertemperaturnetzen,” SWM, Tech. Rep., 2015. [Online]. Available: <https://www.swm.de/dam/doc/geschaeftskunden/fernwaerme/broschuere-fernwaerme-ruecklauftemperatur.pdf>.

### Declaration of Generative AI and AI-assisted technologies in the writing process

During the preparation of this work, the authors used Grammarly to improve language and readability. After using this tool/service, the authors reviewed and edited the content as needed and take full responsibility for the content of the publication.